J|A|C|S ARTICLES

Published on Web 04/26/2010

# Predictions of the $Pt_8Ti$ Phase in Unexpected Systems

Richard H. Taylor,[†,‡] Stefano Curtarolo,[*,‡,§] and Gus L. W. Hart[*,†]

*Department of Physics and Astronomy, Brigham Young University, Provo, Utah 84602, Department of Mechanical Engineering and Materials Science and Department of Physics, Duke University, Durham, North Carolina 27708, and Department of Materials and Interfaces, Weizmann Institute of Science, Rehovot 76100, Israel*

Received March 5, 2010; E-mail: gus.hart@gmail.com; stefano@duke.edu

***Abstract:*** The binary $A_8B$ phase (prototype $Pt_8Ti$) has been experimentally observed in 11 systems. A *high-throughput* search over all the binary transition intermetallics, however, reveals 59 occurrences of the $A_8B$ phase: $Au_8Zn^{\dagger}$, $Cd_8Sc^{\dagger}$, $Cu_8Ni^{\dagger}$, $Cu_8Zn^{\dagger}$, $Hg_8La$, $Ir_8Os^{\dagger}$, $Ir_8Re$, $Ir_8Ru^{\dagger}$, $Ir_8Tc$, $Ir_8W^{\dagger}$, $Nb_8Os^{\dagger}$, $Nb_8Rh^{\dagger}$, $Nb_8Ru^{\dagger}$, $Nb_8Ta^{\dagger}$, $Ni_8Fe$, $Ni_8Mo^{\dagger *}$, $Ni_8Nb^{\dagger *}$, $Ni_8Ta^{*}$, $Ni_8V^{*}$, $Ni_8W$, $Pd_8Al^{\dagger}$, $Pd_8Fe$, $Pd_8Hf$, $Pd_8Mn$, $Pd_8Mo^{*}$, $Pd_8Nb$, $Pd_8Sc$, $Pd_8Ta$, $Pd_8Ti$, $Pd_8V^{*}$, $Pd_8W^{*}$, $Pd_8Zn$, $Pd_8Zr$, $Pt_8Al^{\dagger}$, $Pt_8Cr^{*}$, $Pt_8Hf$, $Pt_8Mn$, $Pt_8Mo$, $Pt_8Nb$, $Pt_8Rh^{\dagger}$, $Pt_8Sc$, $Pt_8Ta$, $Pt_8Ti^{*}$, $Pt_8V^{*}$, $Pt_8W$, $Pt_8Zr^{*}$, $Rh_8Mo$, $Rh_8W$, $Ta_8Pd$, $Ta_8Pt$, $Ta_8Rh$, $V_8Cr^{\dagger}$, $V_8Fe^{\dagger}$, $V_8Ir^{\dagger}$, $V_8Ni^{\dagger}$, $V_8Pd$, $V_8Pt$, $V_8Rh$, and $V_8Ru^{\dagger}$ ($^{\dagger}$ = metastable, * = experimentally observed). This is surprising for the wealth of new occurrences that are predicted, especially in well-characterized systems (e.g., Cu−Zn). By verifying *all* experimental results while offering additional predictions, our study serves as a striking demonstration of the power of the high-throughput approach. The practicality of the method is demonstrated in the Rh−W system. A cluster-expansion-based Monte Carlo model reveals a relatively high order−disorder transition temperature.

## I. Introduction

Binary ordered phases with high stoichiometric ratio compositions (7:1 and higher) are rare.[1,2] Despite the rarity of phases with stoichiometry far from 1:1, however, there is considerable interest in identifying their existence. Beyond the fundamental scientific motivation to characterize the complete ground states of binary systems, it is well known that even small amounts of an alloying agent may result in dramatic material enhancements when ordering occurs (e.g., strength[3,4]). To illustrate this point, consider the case of order-induced hardening in platinum−copper.[5] The addition of 14 atom % Cu in Pt can result in the formation of ordered domains of the type $A_7B$,[6] increasing the hardness in some instances by more than double that of untreated specimens.

Of the few high-stoichiometry phases, the $A_8B$ phase (Pearson symbol tI18 and space group $I4/mmm$,[7] Figure 1) is of particular interest—it forms in systems containing elements from the transition metal group and has potential applications in catalysis, high-temperature electrodes, and jewelry. It was first reported by Pietrokowsky in 1965 in Pt−Ti (hence prototype $Pt_8Ti$[8])[9] and has since been found in 11 metallic systems. In order of discovery, they are $Pt_8Ti$,[9] $Pt_8Zr$,[10] $Ni_8Nb$,[11] $Ni_8Ta$,[12] $Ni_8V$,[13] $Pd_8W$,[14] $Pd_8V$,[15] $Pt_8V$,[7] $Ni_8Mo$,[16] $Pd_8Mo$,[17] and $Pt_8Cr$.[18]

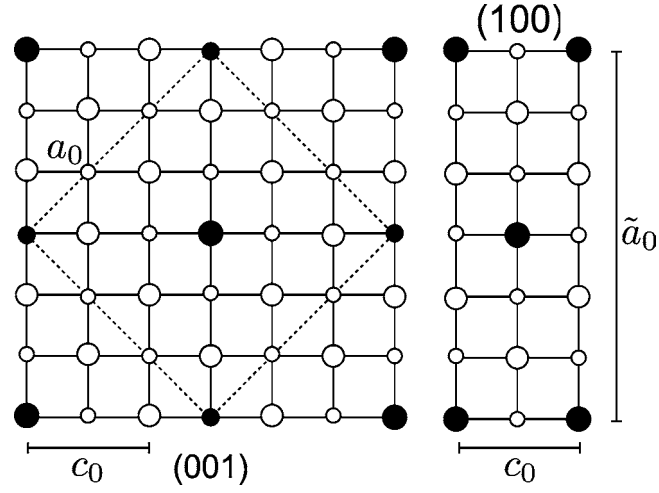


***Figure 1.*** Projections of the $A_8B$ phase along (001) and (100). Atoms sit on face-centered cubic lattice sites, with large circles indicating atoms in the plane of the page and small circles suggesting a displacement $a/2$ perpendicular to the plane. The body-centered tetragonal unit cell is indicated by the dashed lines. A non-primitive face-centered tetragonal cell is outlined by the perimeter.

[†] Brigham Young University.
[‡] Duke University.
[§] Weizmann Institute of Science.

(1) Massalski, T. B., Okamoto, H., Subramanian, P. R., Kacprzak, L., Eds. *Binary alloy phase diagrams*; American Society for Metals: Materials Park, OH, 1990.
(2) Villars, P.; Berndt, M.; Brandenburg, K.; Cenzual, K.; Daams, J.; Hulliger, F.; Massalski, T.; Okamoto, H.; Osaki, K.; Prince, A.; Putz, H.; Iwata, S. *J. Alloys Compd.* **2004**, *367*, 293–297.
(3) Cahn, R. W. Metallurgical Society Conference Series *36*, 1966.
(4) Stoloff N. S., Davies R. G. *Prog. Mater. Sci.* **1966**, *13*.
(5) Carelse, M.; Lang, C. *Scr. Mater.* **2006**, *54*, 1311–1315.
(6) Schneider, A.; Esch, U. Z. *Z. Electrochem.* **1944**, *50*, 290.
(7) Schryvers, D.; Landuyt, J. V.; Amelinckx, S. *Mater. Res. Bull.* **1983**, *18*, 1369–1374.
(8) $Ni_8Nb$ is the prototype in some sources, although its discovery came some years after Pietrokowsky first reported $Pt_8Ti$.
(9) Pietrokowsky, P. *Nature* **1965**, *206*, 291.
(10) Krautwasser, P.; Bhan, S.; Schubert, K. *Z. Metallkde.* **1968**, *59*, 724–729.
(11) Quist, W. E.; van der Wekken, C.; Taggart, R.; Polonis, D. H. *Trans. Met. Soc. AIME* **1969**, *245*, 345–349.

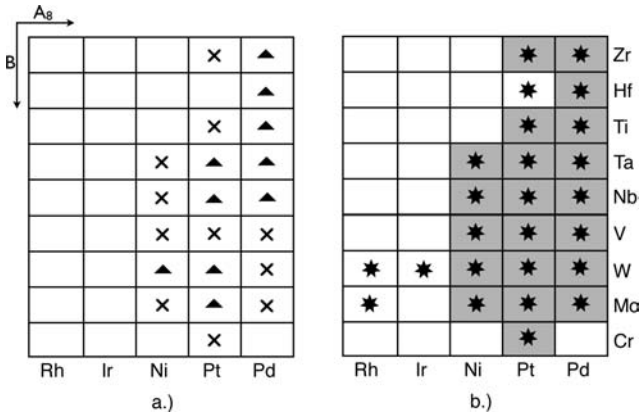


***Figure 2.*** (a) Pettifor-type structure map of the $A_8B$ phase in the Rh, Ir, Ni, Pt, and Pd systems. The concentration-rich elements are listed horizontally. Both axes are labeled by increasing Mendeleev number. Predictions given by Ardell[21] are labeled with a triangle, and experimentally observed systems are labeled with a cross. (b) HT predictions are indicated by a star. Overlap with experiment and predictions is complete (indicated by the shaded region). Our predictions, however, are not limited to these results (e.g., Rh−W).

Systems found to exhibit the $A_8B$ phase are limited to combinations of the transition metals—specifically to group 10 alloyed with group 4−6 (IUPAC nomenclature) elements—indicating a correlation between the localized unfilled d-orbitals and formation of the 8:1 phase. Further, one notes that the elemental phase of the concentration-rich element is face-centered cubic (fcc) in every case, as expected because $A_8B$ is a fcc derivative superstructure.

With these general observations in mind, it was natural to explore the group 9 fcc elements, Rh and Ir, alloyed with group 4−6 elements, as candidate systems. Experimental and theoretical[19] investigation of $A_8B$ has largely been limited to group 10 elements as the concentration-rich constituent, perhaps due to their similarity to platinum and implications of the Pettifor-type structure map.[20]

A structure map of the Pettifor type is shown in Figure 2a. Known $A_8B$ phases and likely stable phases summarized by Ardell[15] are indicated in the diagram. When the candidates are compared with the results of *high-throughput* (HT) calculations (see Methods section), however, several phases (Rh−W, Rh−Mo, Ir−W, Pt−Hf) not included in the Pettifor map are predicted to be thermodynamically stable (Figure 2). Scandium phases ($Pd_8Sc$ and $Pt_8Sc$) were also found (although not shown in the figure), the existence of which is indeed surprising in this light, as the Mendeleev number of Sc is smaller than those of all the rare earths, none of which have been shown to form the $A_8B$ phase.

## II. Methods

In the HT approach, previously unexpected ground states are found by a brute-force search: formation enthalpies are calculated for essentially every crystal structure ever observed in binary metal systems as well as a large number of enumerated derivative superstructures.[22] For this study, the calculations were performed using the AFLOW framework[23−27] based on *ab initio* calculations of the energies using the VASP software.[28] We used projector-augmented wave (PAW) pseudopotentials[29] and the exchange-correlation functionals parametrized by Perdew, Burke, and Ernzerhof[30] for the generalized gradient approximation. The energies were calculated at zero temperature and pressure (thus energies and enthalpies coincide), with spin polarization and without zero-point motion or lattice vibrations (zero-point motion is negligible because we do not consider light elements). All crystal structures were fully relaxed (cell volume and shape, and atomic positions). Numerical convergence to about ∼1 meV/atom was ensured by a high energy cutoff (30% higher than the highest-energy cutoff for the pseudopotentials of the components) and dense 6000 *k*-point Monkhorst−Pack meshes.

The HT search included the 435 binary intermetallics that can be made with transition metals (La included). For each system, the energies of 200 crystal structures were calculated. In addition to the 176 configurations described in ref 23, these included all the symmetrically distinct hexagonal close packed (hcp)-, body-centered cubic (bcc)-, and face-centered cubic (fcc)-based superstructures,[22] with up to four atoms per cell, and the prototypes A5, A6, A7, A8, A9, A11, B20, C36, $D5_{19}$, $Al_2Zr_4$, $Al_3Zr_2$, CdTi, $CuPt_7$, $Cu_3Ti_2$, $Ga_2Hf$, $Ga_4Ni$, $Ga_3Pt_5$, $Ga_4Ti_5$, $Hg_2Pt$, ITl, InTh, LiB-MS1/2,[31,32] $NbNi_8(Pt_8Ti)$, $NiTi_2$, SeTl, and $V_4Zn_5$. The additional prototypes were considered because they are common or related to noble metal alloys.[1,2] We did not consider lattice superstructures with more than four atoms per cell because their number increases enormously. It should also be noted that systems exist which do not conserve the parents' lattice (i.e., Hf−Ti, Hf−Zr[26]).

This procedure gives reasonable results, as shown in ref 23. Here it was shown that the probability of reproducing the correct ground state—if well defined, unambiguous, and present in our list of prototypes—is $\eta_c^* \approx 96.7\%$ ("*reliability of the method*", eq (3) of ref 23). There is no guarantee that the true ground state of a system will be found among the common experimentally observed structures or among small-unit-cell derivative structures. However, even if it is impossible to rule out the existence of an unexpected ground state, this procedure (searching many enumerated derivative structures and exhaustively exploring experimentally reported structures) is expected to give a reasonable balance between HT speed and scientific accuracy to determine the presence of $A_8B$ phases.

## III. Results and Discussion

Following the unexpected HT predictions shown in Figure 2b, the search for systems exhibiting $A_8B$ was extended to all transition metals, including lanthanum. The results of the HT

(12) Larson, J. M.; Taggart, R.; Polonis, D. H. *Metall. Trans.* **1970**, *1*, 485–489.
(13) Moreen, H. A.; Taggart, R.; Polonis, D. H. *J. Mater. Sci.* **1971**, *6*, 1425–1432.
(14) Weaver, L.; Ardell, A. J. *Scr. Metall.* **1980**, *14*, 765–768.
(15) Ardell, A. J.; Janghorban, K. *Phase Transitions During Irradiation*; Applied Science Publishers: London, 1982.
(16) Mayer, J.; Urban, K. *Phys. Stat. Sol. (a)* **1985**, *90*, 469–475.
(17) Mostafa, M. S.; Ardell, A. J. *Mater. Lett.* **1987**, *3*, 67–70.
(18) Nzula, M. P.; Lang, C. I. ; Cockayne, D. J. H *J. Alloys Compd.* **2006**, *420*, 165–170.
(19) Lu, Z. W.; Klein, B. M. *Phys. Rev. B* **1994**, *50*, 5962–5970.
(20) Pettifor, D. *Mater. Sci. Technol.* **1988**, *4*, 675–691.
(21) Pettifor, D. *Met. Alloys: Exp. Theor. Persp.* **1994**, *256*, 93–102.
(22) Hart, G. L. W.; Forcade, R. W. *Phys. Rev. B* **2009**, *80*, 014120.
(23) Curtarolo, S.; Morgan, D.; Ceder, G. *Calphad* **2005**, *29*, 163.
(24) Curtarolo, S.; Morgan, D.; Persson, K.; Rodgers, J.; Ceder, G. *Phys. Rev. Lett.* **2003**, *91*, 135503.
(25) Curtarolo, S.; Hart, G. L. W.; Setyawan, W.; Chepulskii, R. V.; Levy, O.; Morgan, D. *AFLOW: software for high-throughput calculation of material properties*; 2009; http://materials.duke.edu/aflow.html.
(26) Levy, O.; Hart, G. L. W.; Curtarolo, S. *J. Am. Chem. Soc.* **2010**, *132*, 4830.
(27) Levy, O.; Hart, G. L. W.; Curtarolo, S. *Acta Mater.* **2010**, *58*, 2887.
(28) Kresse, G.; Hafner, J. *Phys. Rev. B* **1993**, *47*, 558.
(29) Blochl, P. E. *Phys. Rev. B* **1994**, *50*, 17953.
(30) Perdew, J. P.; Burke, K.; Ernzerhof, M. *Phys. Rev. Lett.* **1996**, *77*, 3865.
(31) Kolmogorov, A. N.; Curtarolo, S. *Phys. Rev. B* **2006**, *73*, 180501(R).
(32) Kolmogorov, A. N.; Curtarolo, S. *Phys. Rev. B* **2006**, *74*, 224507.

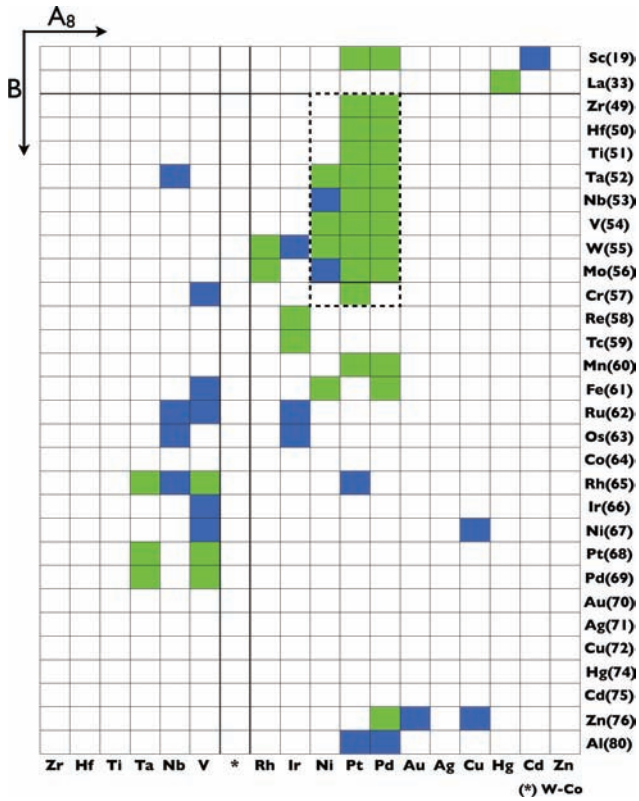


***Figure 3.*** Complete set of $A_8B$ phases predicted by HT calculations. Elements are listed according to the Mendeleev number after Pettifor.[20] Many previously unsuspected candidate systems are revealed, spanning the transition metals and La and Sc. "W−Co" = W, Mo, Cr, Re, Tc, Mn, Fe, Ru, Os, and Co; no ground states at composition $A_8B$ were found in this region.

search indicate thermodynamically stable and metastable (described below) $A_8B$ phases in 59 systems: $Au_8Zn^{\dagger}$, $Cd_8Sc^{\dagger}$, $Cu_8Ni^{\dagger}$, $Cu_8Zn^{\dagger}$, $Hg_8La$, $Ir_8Os^{\dagger}$, $Ir_8Re$, $Ir_8Ru^{\dagger}$, $Ir_8Tc$, $Ir_8W^{\dagger}$, $Nb_8Os^{\dagger}$, $Nb_8Rh^{\dagger}$, $Nb_8Ru^{\dagger}$, $Nb_8Ta^{\dagger}$, $Ni_8Fe$, $Ni_8Mo^{\dagger}$*, $Ni_8Nb^{\dagger}$*, $Ni_8Ta$*, $Ni_8V$*, $Ni_8W$, $Pd_8Al^{\dagger}$, $Pd_8Fe$, $Pd_8Hf$, $Pd_8Mn$, $Pd_8Mo$*, $Pd_8Nb$, $Pd_8Sc$, $Pd_8Ta$, $Pd_8Ti$, $Pd_8V$*, $Pd_8W$*, $Pd_8Zn$, $Pd_8Zr$, $Pt_8Al^{\dagger}$, $Pt_8Cr$*, $Pt_8Hf$, $Pt_8Mn$, $Pt_8Mo$, $Pt_8Nb$, $Pt_8Rh^{\dagger}$, $Pt_8Sc$, $Pt_8Ta$, $Pt_8Ti$*, $Pt_8V$*, $Pt_8W$, $Pt_8Zr$*, $Rh_8Mo$, $Rh_8W$, $Ta_8Pd$, $Ta_8Pt$, $Ta_8Rh$, $V_8Cr^{\dagger}$, $V_8Fe^{\dagger}$, $V_8Ir^{\dagger}$, $V_8Ni^{\dagger}$, $V_8Pd$, $V_8Pt$, $V_8Rh$, and $V_8Ru^{\dagger}$ ($^{\dagger}$ = metastable, * = experimentally observed) (see Figure 3). Thus, previously unsuspected occurrences of the $A_8B$ phase are predicted in 48 systems. Some of the components in the predicted systems come from unexpected places on the periodic table (e.g., Hg−La) compared to the components in the experimentally known 8:1 phases.

Systems in which the $A_8B$ structure is less than 3 meV above or below the tieline defined by adjacent ground states are labeled metastable (indicated by the blue tiles in Figure 3). A definitive statement regarding the existence of a $T = 0$ K ground state at 8:1 stoichiometry is difficult to make in these instances. Energies on the order of several millielectronvolts are small in comparison with the formation enthalpies of stable states in the systems studied, and such small flucations may be due to systematic error in DFT calculations. Regardless of these considerations, however, metastable states are often realizable at finite temperature because of entropic stabilazation. Indeed, certain *experimental phases* (e.g., $Ni_8Mo$) are found to be *metastable* by our quantum mechanical calculations.

The case of $Pt_7Cu$ was introduced at the beginning as an example of material improvement gained by ordering. More

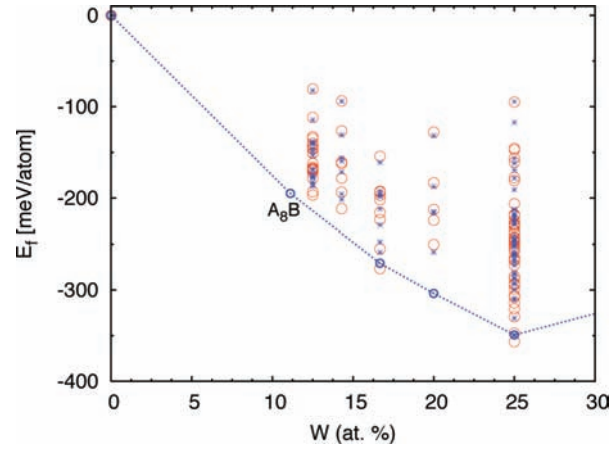


***Figure 4.*** CE input energies calclated from first principles (red, large circles) with cluster expansion predictions (blue, stars). The blue tie line connects the stable structures after a ground state search. For clarity, the ground state search enthalpies are not shown *except* for the stable states, the vertices of the convex hull (blue line). The stable state at $x = 11$ atom % W is the 8:1 structure. Input structures with concentrations between 0 and 25 atom % W were selected because the applicability of an fcc CE approach was established by HT within this range.

noteworthy, however, is the fact that a well-studied system yielded a previously unobserved ordered phase. Pt−Cu is a common jewelry alloy that has been investigated for decades and has been used for more than a century. Despite this, the ordered phase was only observed recently, after the appropriate sequence of annealing and cold working. Thus, one should not discount predicted phases merely because a system is well studied (e.g., Cu−Zn, Cu−Ni). Phases with finite order−disorder transitions may go unnoticed for many reasons, not the least of which is the real limitation imposed by kinetics. Several observed $A_8B$ phases ($Pd_8W$, $Pd_8V$, and $Pd_8Mo$), for example, have only been realized after the introduction of excess vacancies by charged-particle irradiation.[15]

Even so, since all HT quantum mechanical energy calculations were performed at zero temperature, it is possible that some of the predicted $A_8B$ phases will not be observed experimentally. That is, it may be difficult to achieve thermal equilibrium in certain systems. The kinetics will be too slow to observe ordering in reasonable time if the concentration of thermally induced vacancies is too low.

To address this, it is desirable to leverage the synergy of an approach that combines[26] HT with a model that can be extended to finite temperature, such as the cluster expansion (CE). Transition temperatures estimated by CE-based Monte Carlo simulations give an estimate of the likelihood of observing a transition experimentally.

We conducted a CE study, using the UNCLE[33,34] code, on the $A_8B$-forming Rh−W system. The CE was constructed using the energies of structures with concentrations in the range 0−25 atom % W (Figure 4). At higher W concentration, HT results indicate that zero temperature ground states will not form fcc derivative superstructures. Thus, the range of the CE was kept within the limits indicated by the HT results. The validity of this reduction is further shown by noting that the lowest-energy predicted ground state is at 25 atom % W.

(33) Blum, V.; Hart, G. L. W.; Walorski, M. J.; Zunger, A. *Phys. Rev. B* **2005**, *72*, 165113.
(34) Lerch, D.; Wieckhorst, O.; Hart, G. L. W.; Forcade, R. W.; Muller, S. *Modell. Simul. Mater. Sci. Eng.* **2009**, *17*, 055003(19 pp).

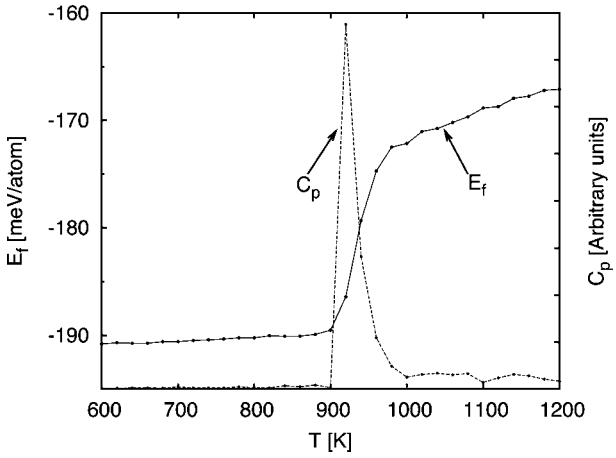


***Figure 5.*** Canonical Monte Carlo results at 11 atom % W in Rh−W. Configurational specific heat is overlaid with finite temperature formation enthalpy. The transition is estimated between 900 and 1000 K.

Quantum mechanical energies used in the construction of the CE were computed on an equivalent *k*-point scheme to reduce systematic error. Rh and W pseudopotentials incorporating the semi-core p electrons with an energy cutoff of approximately 271 eV were used. Input energies, CE predictions, and lowest-energy predictions of the ground state search (including fcc superstructures with up to 10 atoms per unit cell) are shown in Figure 4. A canonical Monte Carlo simulation using the Metropolis algorithm was performed on a $20 \times 20 \times 20$ unit cell with periodic boundary conditions. The results, including the specific heat determined using the familiar statistical relation $\sigma_E^2 = \langle E^2 \rangle - \langle E \rangle^2$, are shown in Figure 5.

CE-based MC modeling revealed an order−disorder transition temperature between 900 and 1000 K in the Rh−W system at 8:1 stoichiometry. Experimental Rh−W phase diagrams show the liquidus line near 2200 K at 11 atom % W. It is then conceivable that the $A_8B$ phase could be produced after the introduction of excess vacancies (via charged particle irradiation[15] or cold working[5]), if not by spontaneous ordering alone.

## IV. Conclusions

In conclusion, using the high-throughput method, the $A_8B$ phase was found in 59 systems, 48 of which are yet unobserved. By verifying experiment and previous predictions while also offering *additional* predictions, our results demonstrate the power of the HT approach in a dramatic fashion. Although it is possible that some of the predicted phases may not be observed experimentally due to kinetic limitations, a CE extension to finite temperatures illustrates that the investigation is not merely academic. In the system Rh−W, the transition was predicted high enough to be realized experimentally. Further investigation is required to determine the extent to which the remaining predicted phases may be seen experimentally.

**Acknowledgment.** We thank Wahyu Setyawan and Ohad Levy for fruitful discussions. Research supported by ONR (N00014-07-1-0878, N00014-07-1-1085, N00014-09-1-0921) and NSF (DMR-0639822, DMR-0650406). We are grateful for extensive use of the Fulton Supercomputer Center at Brigham Young University and Teragrid resources (MCA-07S005). S.C. acknowledges support from the Feinberg Fellowship at the Weizmann Institute of Science.

JA101890K